Displaying morphological and lithological maps: A numerically intensive computing and visualization application

Algorithms for evaluating digital terrain models (DEMs) and elevation moments such as slope, aspect, relief, and curvature are discussed. Significant new applications based on the elaboration and display of such data are presented. The results show that the processed data can be used for environmental protection and to identify topography-dependent natural-disaster hazards.

Introduction

Information extracted from dense-grid digital elevation models, combined with lithological information derived from remotely sensed or field data, can be used in terrain classification and geomorphometric studies [1, 2]. The arrangement of data on a regular grid permits the data to be easily combined with satellite images.

In this paper we address the study and presentation of terrain characteristics as a useful application of image processing and computer graphics in support of environmental protection and the quantitative evaluation of hazardous sites. An important application is the assessment of volcanic areas for which morphometric information provides a powerful indicator of the geologic history of the region and supports the development of dynamic models that simulate topography-dependent phenomena: mud slides,

debris flow, ash flow, lava flow, etc.

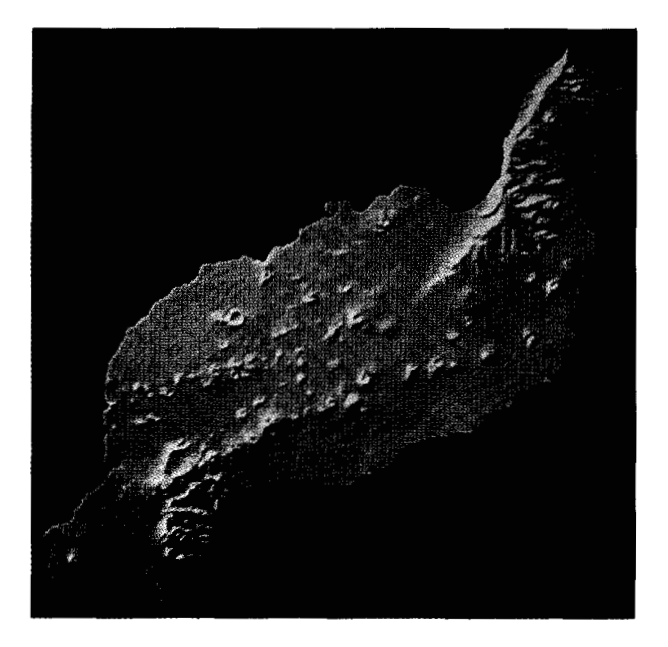
Geomorphometric maps (DEMs and elevation moments such as aspect, slope, curvature, and relief) have been obtained for several areas and are displayed in orthogonal and isometric views in combination with remote-sensing information.

Interpolation techniques based on fractals are analyzed, focusing attention on the statistical implications of these techniques for the numerical simulation of flowing or creeping water, mud, and lava.

Digital elevation models

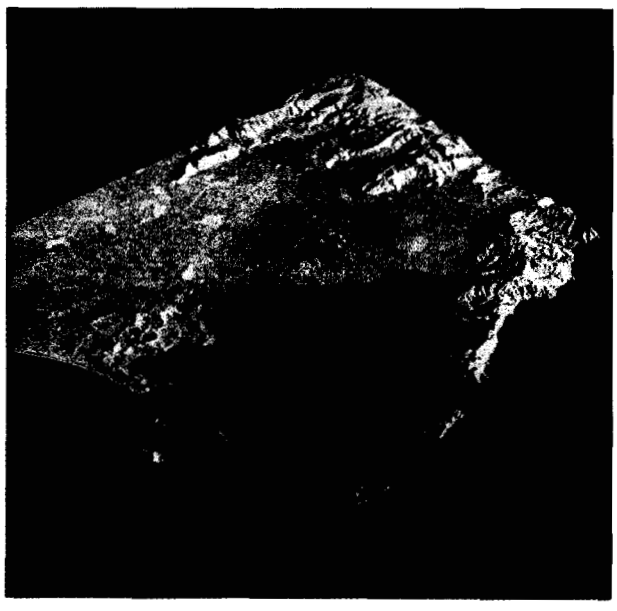
Elevation information on a regular grid can be obtained directly from stereo digital images [3, 4]. If elevation data are available only on a sparse or irregular basis, data on a regular mesh must be derived. Many techniques are available for obtaining such data: e.g., polynomial

**Copyright 1991 by International Business Machines Corporation. Copying in printed form for private use is permitted without payment of royalty provided that (1) each reproduction is done without alteration and (2) the Journal reference and IBM copyright notice are included on the first page. The title and abstract, but no other portions, of this paper may be copied or distributed royalty free without further permission by computer-based and other information-service systems. Permission to republish any other portion of this paper must be obtained from the Editor.





Perspective shaded image "draped" over a digital elevation model for Lanzarote Island. Pixel resolution is 40 m; the vertical scale is magnified four times with respect to the horizontal one.



Ballina 2

Perspective view of Vesuvius (Italy). Landsat bands 1, 3, and 7 are used for color definition. Pixel resolution is 120 m.

interpolations, splines, kriging techniques [5]. In principle, stochastic techniques (such as kriging) are preferred to deterministic methods (linear interpolations, splines) because they ensure the optimization of the estimate and provide error evaluation. In any case, whatever the technique used, control points must be randomly distributed to ensure an unbiased reconstruction. **Figures 1** and **2** show DEMs of Lanzarote Island (Canary Islands, Atlantic Ocean) and the Vesuvian area (Italy) reconstructed by a kriging technique (the source data were obtained from maps at scales of 1:10 000 and 1:50 000. The pixel resolutions are 40 m for Lanzarote and 120 m for the other images; the average error on computed elevations is in the range of 3-10 m.

When input points are clustered, as for example when digitized along isolines from topographic maps, a terrain surface can be rendered as a network of planar facets, providing a satisfactory triangulation (for example the Delaunay one) of the initial set of points (Figure 3). Data on a regular grid can then be readily obtained by linear interpolation [6].

Either stereo images or sparse control points are used for DEM evaluation; there is a maximum meaningful spatial resolution (that is, a minimum step of the mesh) related to change in elevation in the first case and to density of control points in the second case [8]. The use of a smaller step size would involve the calculation of redundant or misleading information.

A DEM can be interpolated to obtain greater definition (but it is important to note that a mathematical interpolation does not improve elevation information from a metric point of view [9]). An interesting interpolation technique preserving the intrinsic characteristics of real terrain shape, that is, the statistical properties of the given data, is based on fractals [10]. According to this method, the elevation surface $f(\bar{x})$ in the point $\bar{x} = (x, y)$ is assimilated to a fractional Brownian function for which the following relation holds:

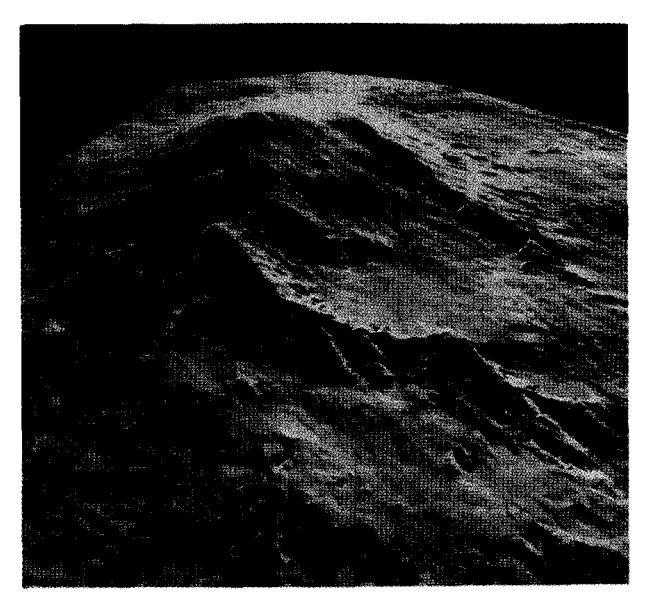
$$Pr\left[\frac{f(\vec{x} + \Delta \vec{x}) - f(\vec{x})}{\|\Delta \vec{x}\|^H} < t\right] = F(t),\tag{1}$$

where F(t) is the cumulative distribution function of a zero-mean Gaussian distribution $N(0, \sigma^2)$:

$$F(t) = \int_{-\infty}^{t} 1/[(2\pi)^{1/2} \sigma] \exp \frac{-s^2}{2\sigma^2} ds.$$

The parameter H is a constant in the range 0-1. Following the notation of Pentland [11], Equation (1) can be rewritten as

$$E[|f(\vec{x} + \Delta \vec{x}) - f(\vec{x})|] \|\Delta \vec{x}\|^{-H} = (2/\pi)^{\nu_2} \sigma,$$
 (2)



Gigura 8

Perspective view of Mt. Etna volcano (Italy). obtained by the Delaunay triangulation of 70 000 points. The visualization was developed using the GALAXY package [7].

or, equivalently,

$$\log E[|f(\hat{x} + \Delta \hat{x}) - f(\hat{x})|] - H \log ||\Delta \hat{x}||$$

$$= \log \left[\left(\frac{2}{\pi} \right)^{1/2} \sigma \right]. \quad (3)$$

In Equations (2) and (3), $E[\cdot]$ denotes the expected value. Equation (3) suggests that, from real terrain data, it is possible to compute fractal characteristics (H and σ). When the points $\log E[|f(\hat{x} + \Delta \hat{x}) - f(\hat{x})|]$ versus $\log \|\Delta \hat{x}\|$ (obtained from real data) are approximated by a straight line, the slope gives H, and the intercept is equal to $\log [(2/\pi)^{V_2} \sigma]$. Provided that fractal characteristics do not vary in the scale of interest and that the points (i, j) such that both i and j are odd numbers have already been determined, a recursive four-neighbor interpolation technique is

$$f(i,j) = (1/4)[f(i-1,j-1) + f(i+1,j-1) + f(i-1,j+1) + f(i+1,j+1)] + (1-2^{2H-2})^{\nu_1} \|\Delta x\|^H \sigma \cdot Gauss$$
 (4)

if i and j are both even numbers, and then

$$f(i,j) = (1/4)[f(i,j-1) + f(i-1,j) + f(i+1,j) + f(i,j+1)] + 2^{-H/2} (1 - 2^{2H-2})^{V_2} ||\Delta x||^H \sigma \cdot Gauss$$
 (5)

if only one of i and j is an even number. $\|\Delta x\|$ is the grid step. Gauss indicates a Gaussian random variable with zero mean and unit variance. We later show that fractal DEMs can be used for statistical modeling of topography-dependent phenomena.

Geomorphometric features can be computed from DEMs. The principal geomorphometric features are terrain slope, aspect, relief, and curvature. A common definition of slope and aspect is based on the use of the partial derivatives of the elevation values z with respect to x (east/west) and y (north/south) directions. The partial derivatives can be determined using two 3×3 first-order filters (Sobel operators). Slope and aspect are then

$$slope = \tan^{-1} \left\{ \left[\left(\frac{\partial z}{\partial x} \right)^2 + \left(\frac{\partial z}{\partial y} \right)^2 \right]^{\frac{1}{2}} \right\}; \tag{6}$$

$$aspect = \tan^{-1} \left[\left(\frac{\partial z}{\partial z} \right) / \left(\frac{\partial z}{\partial y} \right) \right]. \tag{7}$$

This approach essentially fits a second-order surface to the 4-adjacent neighborhood following a minimum mean-squared error criterion. This method involves attributing characteristics of the mathematical surface to the terrain characteristics. Another approach involves slope; slope is simply the direction of water flow to or from the current point: More exactly, it is the difference in elevation divided by the step of the grid.

A combination of aspect and slope can be visualized by means of a shaded image. The shading values represent an estimate of direct solar illumination and a diffuse component. Shadowed terrain receives only diffuse radiation and may have a negative incidence value. A formula to compute shading is

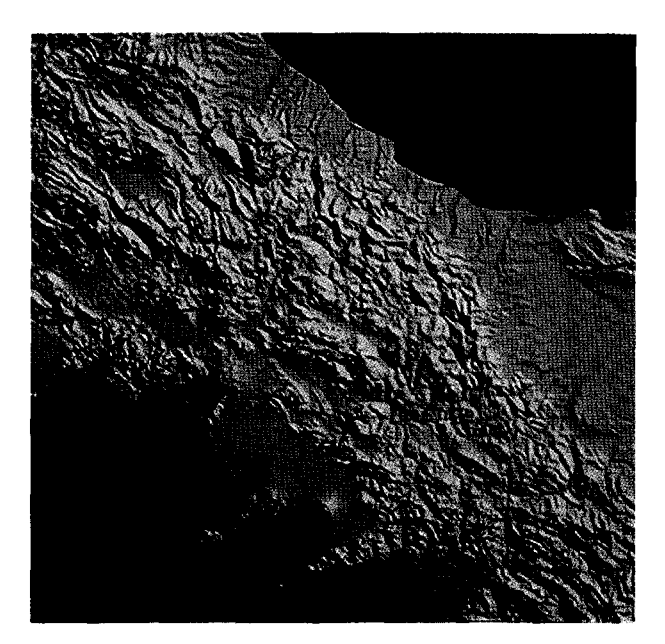
Incidence =
$$\cos(slope) + \sin(slope)$$

 $\cdot \cot(S_E) \cdot \cos(T_A - S_A), \quad (8)$

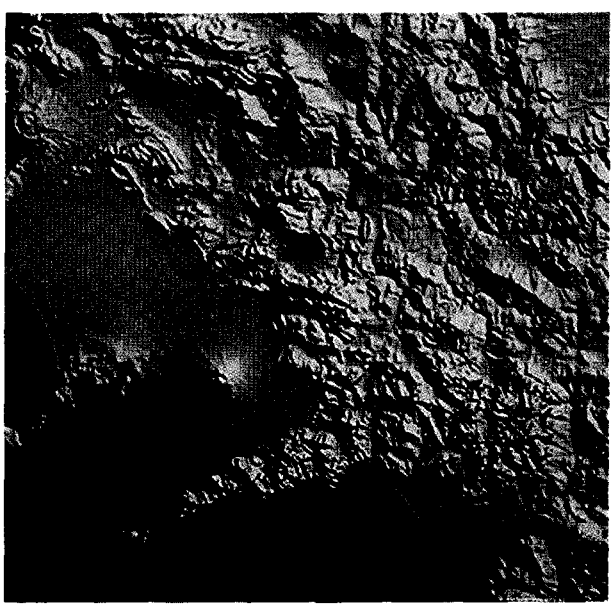
where $S_{\rm E}$ is sun elevation, $T_{\rm A}$ is terrain aspect, and $S_{\rm A}$ is sun azimuth.

Figure 1 and Figures 4 and 5 show shaded images of DEMs. Pixel resolution for the first image is 40 m; for the second, 240 m [12, 13]; and for the third, 120 m. Relief is obviously related to vertical extent. Following Evans [14], a measure of relief can be obtained by the standard deviation of elevation. By this definition, relief also provides an estimate of terrain roughness.

Another important terrain characteristic is local surface convexity: the rate of change of slope or the second derivative of elevation [14]. The calculation is straightforward using best-fitting techniques or nearest neighbors.



Shaded image of central Italy. Pixel resolution is 240 m. Alignment of the Apennines is clearly visible.



Floure 5

Shaded image of Campania area (Italy). Pixel resolution is 120 m. The volcano at the bottom of the image is Vesuvius; that at the top left is Roccamonfina.

Remotely sensing data

For geological applications, an important source of information other than DEMs is remotely sensed data, in particular those data collected by the Thematic Mapper sensors on board the U.S. Landsat 4 and Landsat 5 satellites. A full scene obtained by these sensors has dimensions of 6920 samples by 5760 lines and covers an area of about 185 × 185 km with a spatial resolution of 30 m (120 m in the thermal infrared band); it consists of seven spectral bands located from the visible to the thermal infrared region. Band 1 (0.45-0.52 μ m) can be used to discriminate soil, vegetation, and water; band 2 $(0.52-0.60 \mu m)$ and band 3 $(0.63-0.69 \mu m)$ emphasize vegetation discrimination; band 4 (0.76–0.90 μ m) and band 5 (1.55–1.75 μ m) are important for crop identification and land-water contrast; band 6 (10.4-12.5 μ m) is a thermal infrared band; and band 7 (2.08–2.35 μ m) is important for lithological discrimination.

In the extraction of visual information, color images are generally displayed by selecting three of the available seven bands for red-green-blue (RGB) or intensity, hue, saturation (IHS) color presentation. To avoid the limitation of displaying only three bands of the available seven bands at a time, and to visualize the maximum amount of information, a transformation to principal components is often adopted [15, 16]. This transformation is useful because multispectral images

frequently exhibit a high degree of correlation among spectral bands. The transformation produces a new set of component images that are not correlated. It is possible to order the principal-component images by decreasing the values of the corresponding eigenvalues, which reduces the actual number of bands (the highernumbered bands contain less information). In Table 1, the band correlation matrix, the principal components (eigenvectors), and the eigenvalues are reported for the TM Landsat scene of the Phlegraean Fields (near Naples, Italy) on January 1, 1983 [17]. As can be seen from the table, the correlation of TM band 5 with bands 4 and 7 is 0.86 and 0.93, respectively, while band 1 is relatively uncorrelated with band 5 but shows a high correlation, 0.69, with band 2. One can thus expect a degree of success with principal-component processing. The highest-numbered principal-component bands have a high noise content. This is expected; a simple computation shows that the first three components contain 82% of the original variance (the percent variance of component i is defined as the ratio of the ith eigenvalue to the sum of all the eigenvalues). Figure 6(a) shows the Phlegraean Fields with an RGB display of the first three principal components of the TM Landsat scene of January 1, 1983. Eruptive centers and cones are clearly visible. The most remarkable tectonic element is the northern ridge of the Caldera Flegrea, a structure created

Table 1 Results of principal component processing of Phlegraean Fields Landsat scene.

			Means			
59.302	21.835	20.615	23.853	22.893	97.671	11.774
		,	Standard deviation.	s		
4.603	2.532	3.967	11.261	13.213	7.044	6.924
			Eigenvalues (E_i)			
35.67	39.04	24.71	16.22	2.77	1.94	0.92
			Eigenvectors			
-0.0368	-0.5970	0.3341	0.4577	-0.2926	-0.4246	-0.2349
0.0601	0.2736	0.1391	0.2336	0.0244	0.2309	0.8909
0.1528	0.3678	0.0391	0.1943	0.2933	0.7542	-0.3838
0.5510	-0.4735	0.5828	0.2758	0.2179	-0.0865	-0.0387
0.6881	0.1968	-0.0774	-0.4106	-0.5511	0.0908	0.0044
-0.2910	0.1610	0.6918	-0.6293	0.0805	0.0727	0.0033
0.3296	0.3765	-0.2078	-0.2398	0.6856	-0.4202	0.0476
			Correlation matrix	;		
1.000	0.692	0.413	-0.128	-0.222	0.268	0.023
0.692	1.000	0.808	0.342	0.450	-0.246	0.534
0.413	0.808	1.000	0.553	0.738	-0.521	0.813
-0.222	0.342	0.553	1.000	0.863	-0.670	0.696
-0.128	0.450	0.738	0.863	1.000	-0.725	0.927
0.268	-0.246	-0.511	-0.670	-0.725	1.00	-0.67
0.029	0.534	0.813	0.696	0.928	-0.67	1.000
Band 1	Band 2	Band 3	Band 4	Band 5	Band 6	Band 7

about 35 000 years ago by the ground sinking following a huge pyroclastic eruption. Also clearly visible in Figure 6 are the belt of hills surrounding the Caldera: Monte di Procida, Cuma, S. Severino, Punta Marmolite, and Collina dei Camaldoli; and the volcanic and volcanotectonic structures of the post-Caldera period: Averno-Monte Nuovo to the west, and Cigliano-Senga-Astroni-Solfatara-Agnano Monte Spina to the east.

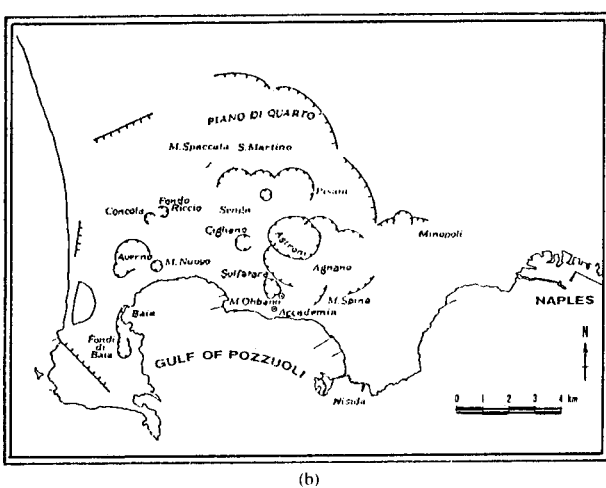
Lithological features in remote-sensing images can be obtained by a process of classification. Classification is a computationally intensive operation for converting multiple source images into a single information image, in such a way that each category or class of information has a separate intensity. In our case, objects are pixels in the image, and categories are water, vegetation, urban area, rock types, etc. The purpose of the classification process is to build a geological map of an area for geological analysis and for hazard prediction and warning. An accurate classification process (the Bayesian approach) has been applied to the Mt. Etna region of Italy. Mt. Etna is the most active volcano in Italy; it is about 40 km in basal diameter and has a height of just over 3000 m. Figures 7 and 8 show a TM Landsat scene of Mt. Etna on May 19, 1984, and the corresponding segmented image. Comparison of an existing geological

map of the Etna region with the processed images from Landsat TM data shows the good results that can be achieved with image-segmentation techniques: Different lithological units are clearly distinguished by different colors.

Terrain analysis

The computation and display of scene characteristics such as elevation, slope, aspect, relief, and curvature, combined with information from remote-sensing data, is a very powerful method for terrain analysis. If heterogeneous source data are used, a registration operation is required; that is, a geometrical transformation must be applied to one of the two images in order to align or register it with the other image. Registration comprises two steps: A mathematical deformation model is computed using control points (that is, features whose location is known in both the images), and then, by using the model, the registered image is generated from the warped one [18, 19]. Control points can be found manually and automatically. In the first case, the user identifies the points by displaying the two images; in the second case, the user again specifies two points to be interpreted—the first as an exact location (the center of a window), and the second as the





(a) RGB display of the first three principal components of the TM Landsat scene of the Phlegraean Fields (near Naples, Italy) on January 1, 1983. (b) Map of the Phlegraean Fields area.

center of a search area which contains the control point. The exact location in the search area is computed as the point of maximum correlation of the window within the search area. Obviously, the process can be further automated by choosing the full image as search area.

The analysis of volcanic regions is the primary focus in this investigation. The information required for computation and presentation includes

1. Remotely sensed images (preferably principalcomponent images) in RGB and IHS.



Figure 7

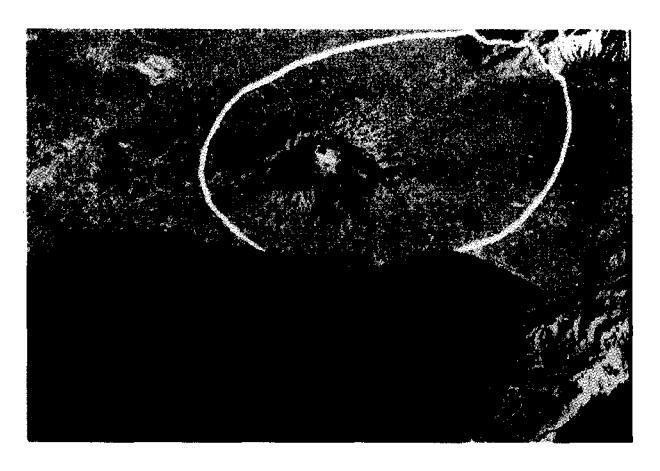
Image of Mt. Etna volcano developed from TM Landsat bands 4. 5, and 7. Scene of May 19, 1984.



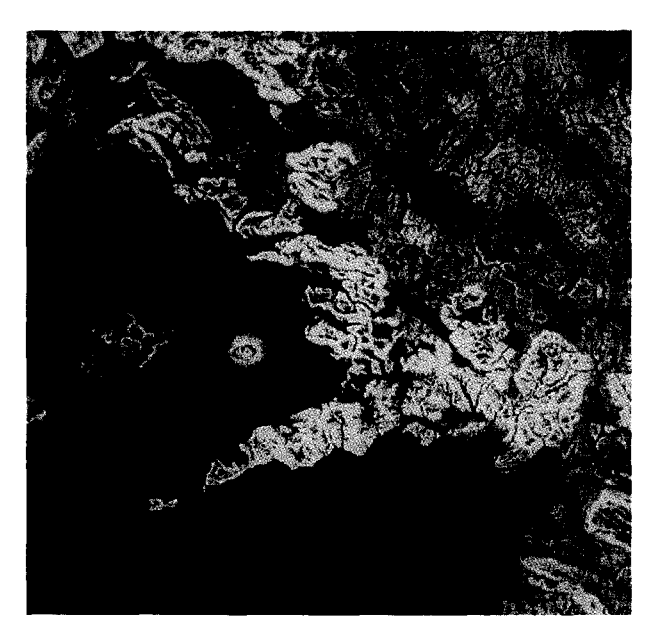
Figure 8

Segmented image obtained starting from image of Figure 7.

- 2. Classified remotely sensed images for outlining different lithological units.
- 3. Elevation and moments of the distribution of elevation and correlation matrices between slope and



Landsat image "draped" over a DEM for Vesuvian area (Italy). The yellow line around the volcano encloses an area with a probability higher than 10% of receiving an ash fall deposit greater than 100 kg/m² if Vesuvius should erupt. Orange color indicates inhabited regions.



Elativa 10

"Slope" image of Campania region (Italy) with a pixel resolution of 120 m. Slope direction is used for hue definition, while slope magnitude defines intensity and saturation.

relief for quantifying the role played by topography in past and future eruptions.

4. Slope information for modeling topography-dependent phenomena.

- Shaded images for outlining the distribution of morphologic units such as faults, ridges, craters, and cones.
- Combined information from past lava flows (derived from remote-sensing data) and elevation, slope, and soil roughness.
- 7. Combined information from slope and vegetation-covered soil for quantifying the possibility of sliding phenomena (landslides, mud flows, avalanches).
- 8. Combined information from numerical-simulation models, remotely sensed data, and DEMs for identifying hazardous sites.

Software has been developed to compute and display this information. In particular, multiple images are displayed by using 3D oblique views: One to three images (Landsat data, shading images, segmented images, correlation matrices) are used as color sources, and another image (mainly elevation) is used to support 3D projection processing [19, 20]. By varying the zenith and the azimuth angles, different perspective views of the same area can be computed and displayed; by changing the vertical scaling factor, an exaggeration of the elevation can be obtained in order to enhance ground features. These possibilities allow detailed analysis and study of the structural features of the earth's surface. Figures 1-5 and Figure 9 show some results. For example, for Lanzarote (the Canary Islands), a shaded image, "draped" in a 3D perspective view over exaggerated topography, allows the outlining of morphological features and gives an insight into the geological history of the island. In particular, the rotation of the eruptive fissures and of the main fractures of the island is easily identifiable and is used to correlate distension axes and volcanic cones.

Another technique for merging information is to use RGB and IHS codification for display. Figure 10 shows a "slope" image of the region of Campania, Italy (pixel resolution 120 m). Slope direction is used for hue definition, while slope magnitude supplies values for intensity and saturation.

Figure 9 and Figure 11 show combined information from remotely sensed data and output from physical-numerical models to identify hazardous sites. In Figure 9, the curve encloses an area which has a probability of an ash-fall deposition greater than 100 kg/m^2 if the Vesuvius volcano should erupt [21]. The orange color indicates inhabited regions. Figure 11 shows a risk map ($risk = hazard \times value \times vulnerability$) [22] for the same eruption of Vesuvius. Vulnerability is taken equal to 1, hazard is deduced from suitable models simulating volcanic ash-fall phenomena, and value is taken equal to the density of inhabited areas, as derived by the segmentation of Landsat images [21].

Data stored on a regular mesh (such as in a DEM) allow for the extraction of information needed for physical-numerical models simulating topography-dependent phenomena. Figure 12 shows the results of a model simulating debris flow. Such data could be utilized to identify hazards from a dam breaking or from a volcanic lahar (a huge volume of mud and water resulting from ice melting due to volcanic eruptions and/or from mobilization by a rain of loose ash accumulated on the volcano slope).

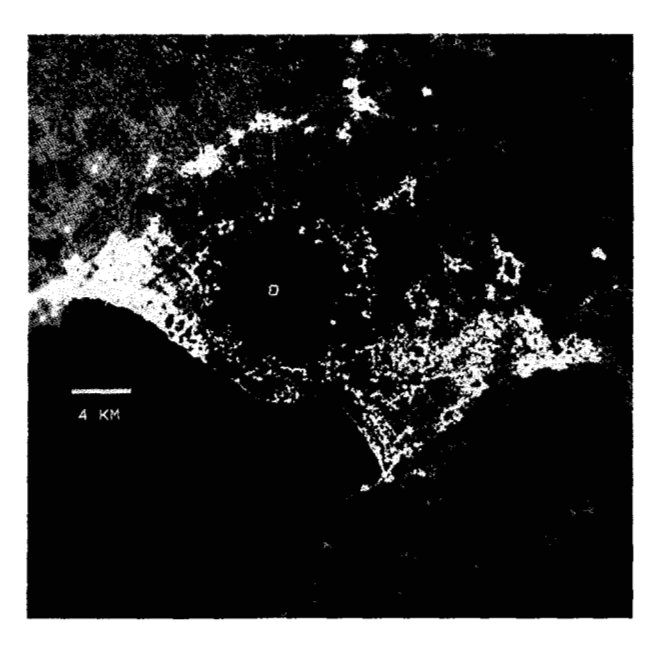
The spatial resolution of a DEM and the error on elevations must be related to the resolution of the model simulating the topography-dependent phenomenon. For example, if a lava flow is sensitive to an obstacle of a few meters, the error elevation must be one order of magnitude smaller. The fractal approach outlined in the first paragraph of this paper can provide help when the resolution of the DEM is not sufficiently dense for simulation purposes. By using fractal interpolation to build surfaces with the desired resolution, the corresponding model output can be evaluated, and the distribution of results provides statistical information on the possible paths.

For example, **Figure 13** shows the results obtained by assuming a very simple model (path of maximum slope). For each fractal-interpolated surface, a line of maximum slope can be derived (with the same starting point). The area enclosed by the two extreme lines identifies hazardous sites. The number of topographies (and thus of lines) to be derived is related to the distribution of the paths. A good criterion to satisfy is that the number of lines intersecting intervals cut along a circle with its center at the starting point be equal to $n^{1/2}$, where n is the number of lines. The size of the intervals depends on the accuracy required to identify the hazard of interest.

The results obtained from 10 000 simulations are displayed in **Figure 14**, which shows lava outflows from multiple vents. Different colors represent different probabilities of lava invasion. A sensitivity analysis shows changes of less than 1% with respect to the case of 1 000 000 simulations. Each "lava flow path" has a maximum allowable length, related to vent quote, according to an empirical law based on field observations.

Conclusions

The derivation of quantitative terrain data such as geomorphometry from digital elevation grids is a fundamental step in terrain analysis. Remote sensing of data provides important information for use in terrain classification. This paper has summarized some of the general image-processing and visualization methods that have been developed and applied to support this discipline. These techniques demonstrate the benefit of



30073

Risk map for the eruption mentioned in Figure 9. With risk values ranging from 0 to 100, light green color indicates a risk value lower than 5, yellow from 5 to 10, red from 10 to 20, and violet greater than 20. A circle indicates the Vesuvius volcano crater.

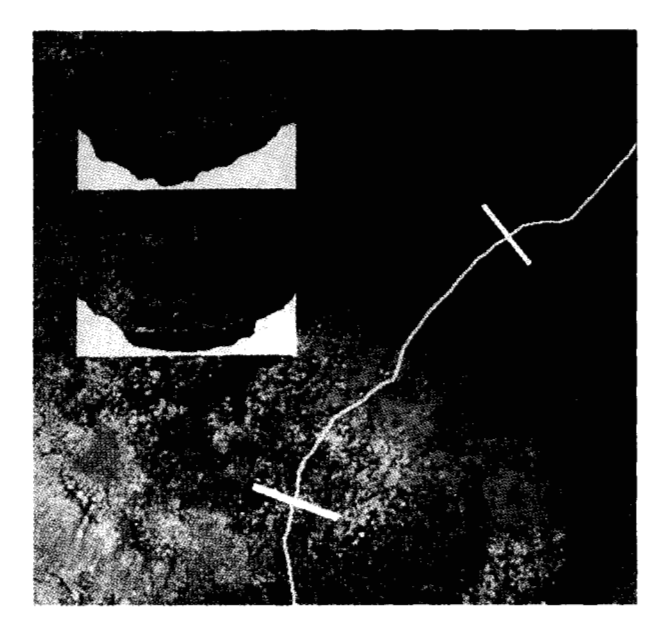


Figure 1

Flow of mud along a line of maximum slope. Two exaggerated profiles of topography and of water level are shown at the top left of the image.



Paths of maximum slope with the same initial point obtained by creating different fractal-interpolated surfaces. The results are depicted in perspective.

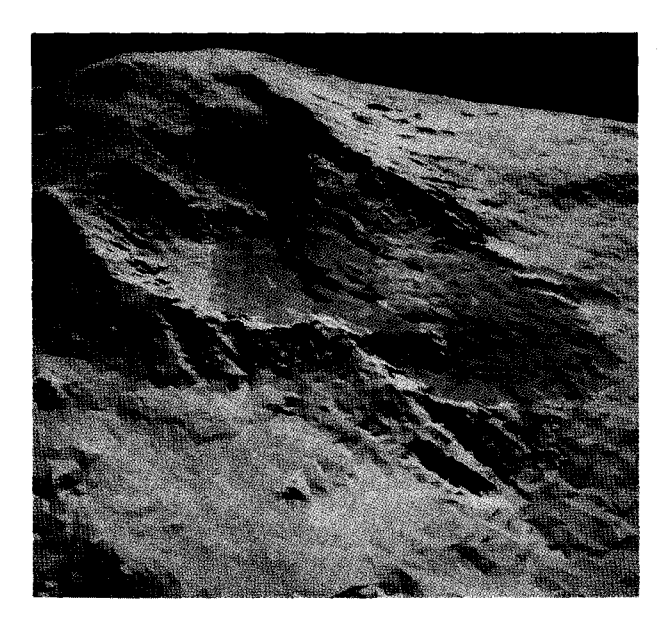


Figure 14

Simulation of lava outflows from multiple vents. Different colors represent different probabilities of lava invasion from a given vent. Data visualization was developed using the GALAXY package [7].

multi-image processing and presentation for visualization and information extraction. Specific applications to volcanic regions have provided very interesting and promising results.

References

- R. G. Craig, "Criteria for Constructing Optimal Digital Terrain Models," Applied Geomorphology, No. 11, R. G. Craig and J. L. Croft, Eds., Allen & Unwin, London, 1983.
- S. E. Franklin, "Geomorphometric Processing of Digital Elevation Models," Computers & Geosci. 13, No. 6, 603–609 (1988).
- D. Rosenholm, "Multi-Point Matching Using the Least-Squares Technique for Evaluation of Three-Dimensional Models," Photogramm. Eng. & Remote Sensing 6, 621-626 (1987).
- D. J. Gugan and I. J. Dowman, "Topographic Mapping from SPOT Imagery," *Photogramm. Eng. & Remote Sensing* 10, 1409-1414 (1988).
- M. T. Pareschi, "Earth Imaging and Data Processing for Mapping and Analysis," *Digital Signal Processing*, V. Cappellini and A. G. Costantinides, Eds., Elsevier Science Publishers, Amsterdam, 1987, pp. 916-921.
- G. Macedonio and M. T. Pareschi, "An Algorithm for the Triangulation of Arbitrarily Distributed Points, Application to Volume Estimate and Terrain Fitting," Computers & Geosci., in press.
- C. A. Pickover, "GALAXY: A Versatile Visualization Program for a Graphics Supercomputer User's Manual (Version 1)," Research Report RC-14570, IBM Thomas J. Watson Research Center, Yorktown Heights, NY, 1989.
- 8. A. E. Balce, "Determination of Optimum Sampling Interval in Grid Digital Elevation Models (DEM) Data Acquisition," *Photogramm. Eng. & Remote Sensing* 3, 323–330 (1987).
- P. Yoeli, "Digital Terrain Models and Their Cartographic and Cartometric Utilization," Cartograph. J. 20, 17-22 (1983).
- N. Yokoya, K. Yamamoto, and N. Funakubo, "Fractal-Based Analysis and Interpolation of 3D Natural Surface Shapes and Their Application to Terrain Modeling," Computer Vision, Graphics & Image Processing 46, 284-302 (1989).
- A. P. Pentland, "Fractal-Based Description of Natural Scenes," IEEE Trans. Pattern Anal. & Machine Intell. PAMI-6, 661–674 (1984).
- M. T. Carrozzo, A. Chirenti, D. Luzio, C. Margiotta, and T. Quarta, "Data Based on Mean Height Values for the Whole Italian Landmass and Surrounding Areas: Determining and Statistical Analysis," *Boll. Geod. e S. Aff.* 44, 37-56 (1985).
- M. Poscolieri and G. Onorati, "A Quantitative Geomorphology Study of Main Carbonate Massifs on Central and Southern Apennines on a Digital Elevation Archive," Proceedings of the International Geoscience and Remote Sensing Symposium, Edinburgh, Scotland, 1988, Cat. No. 88CH 2497-6, IEEE Service Center, Piscataway, NJ, pp. 1653-1654.
- I. S. Evans, "General Geomorphometry, Derivatives of Altitude and Descriptive Statistics," Spatial Analysis in Geomorphology, R. J. Chorley, Ed., Methuen, London, 1972.
- R. Bernstein, "Digital Image Processing of Earth Observation Sensor Data," *IBM J. Res. Develop.* 20, 40–57 (1976).
- R. Bernstein, J. B. Lotspiech, H. J. Myers, H. G. Kolsky, and R. D. Lees, "Analysis and Processing of Landsat-4 Sensor Data Using Advanced Image Processing Techniques and Technologies," *IEEE Trans. Geosci. & Remote Sensing GE-22*, 192-221 (1984).
- M. T. Pareschi, "An Image Processing System for Geological Applications in Remote Sensing," Computing Tools for Scientific Problem Solving, A. Miola, Ed., Academic Press, Inc., New York, 1990, pp. 165-189.
- R. Bernstein and W. A. Hanson, "Advances in Landsat Image Processing and Mapping," Sensor Design Using Computer Tools II, SPIE 550 (1985).
- W. Niblack, An Introduction to Digital Image Processing, Strandberg, Denmark, 1985.

- M. T. Pareschi and R. Bernstein, "Modeling and Image Processing for Visualization of Volcanic Mapping," *IBM J. Res. Develop.* 33, 406–416 (1989).
- F. Barberi, G. Macedonio, M. T. Pareschi, and R. Santacroce, "Mapping the Tephra Fallout Risk: An Example from Vesuvius, Italy," *Nature* 344, 142–144 (1990).
- 22. F. Barberi and F. Gasparini, "Volcanic Hazards," Bull. Int. Assoc. Eng. Geol. 14, 217-232 (1976).

Received November 6, 1989; accepted for publication November 30, 1990

Franco Barberi University of Pisa, Department of Earth Science, Via Santa Maria 53, I-56100 Pisa, Italy. Professor Barberi is a professor of volcanology on the Faculty of Sciences at the University of Pisa and president of the National Group for Volcanology of the Italian National Research Council. In 1975 he was the first recipient of the scientific Wager Prize, awarded by the International Association of Volcanology. His research, initially directed toward understanding the fundamental nature of the volcanic process, has moved in recent years toward the mitigation of natural hazards and the development of approaches for the use of geothermal energy. From 1976 to 1986 Professor Barberi was the director and principal investigator of the Italian Geodynamics Project, which conducted research on the assessment and mitigation of volcanic and seismic hazards. Under his leadership the Project developed superior methodologies for hazard assessment and improved physical and chemical monitoring networks for the study of eruption precursors. Since 1988 he has been the chairman of the Volcanology Network of the European Science Foundation. In the field of geothermal energy, in cooperation with the Latin American Energy Organization (OLADE), Professor Barberi contributed to the definition of a rapid and low-cost methodology for geothermal exploration in volcanic regions, which has since been successfully applied in several Latin American countries. In the field of hazard mitigation, he and his coworkers have in recent years obtained results of international importance in the physical modeling of active volcanoes and the prediction and automatic simulation of eruptions. Professor Barberi has also promoted many other international exchanges in volcanology research, both in Europe and worldwide. In 1985 he led an Italian mission to the Nevado del Ruiz volcano in Colombia, and issued an unheeded warning of the dangerous state of the volcano, whose eruption three weeks later killed 25 000 people.

Ralph Bernstein IBM Palo Alto Scientific Center, 1530 Page Mill Road, Palo Alto, California 94304. Mr. Bernstein is a Senior Technical Staff Member and manager of the Image Science and Applications Department at the IBM Palo Alto Scientific Center. He has a B.S. degree in electrical engineering from the University of Connecticut and an M.S. degree in electrical engineering from Syracuse University. Mr. Bernstein has been involved in image science, applications, and systems development since 1972. His other application experience includes systems simulation and analysis studies for aircraft and submarine navigation and control, satellite systems studies, geophysical data processing, and advanced control systems design. He was responsible for developing the first computerized shipboard oceanographic data acquisition, processing, and control system. Mr. Bernstein was a principal investigator on the NASA Landsat satellite program in 1972-1975 and again in 1982-1985. He developed advanced algorithms and computer programs under these investigations and made significant contributions to the field of image processing. His current interests include visualization and supercomputing, in particular medical, astronomical, and geophysical image processing. Mr. Bernstein edited the IEEE Press Book Digital Image Processing for Remote Sensing, has contributed to several other books on geoscience and related subjects, and has numerous other publications in geoscience, automatic control,

systems simulation, digital image processing, navigation, and oceanography. He served as Chief Imagery Consultant to the National Geographic Society on the publication of their book, Atlas of North America—Space Age Portrait of a Continent. He holds a patent on digital filtering and has several published invention disclosures. Mr. Bernstein is a past member of the Space Science Board and the Space Applications Board of the National Academy of Sciences, and he has been a consultant to NASA. He is also the Chairperson of the IBM Pattern Recognition and Image Processing Interdivisional Technical Liaison group. He has received the NASA Medal for Exceptional Scientific Achievement, the NASA Public Service Medal, the University of Connecticut Distinguished Alumni Award, an IBM Outstanding Contribution Award, the IBM General Manager's Award for Significant Achievement, and the Tau Beta Pi Eminent Engineer Award, Mr. Bernstein is a Fellow of the Institute of Electrical and Electronics Engineers and a member of the American Society of Photogrammetry and Tau Beta Pi.

Maria Teresa Pareschi IBM Pisa Scientific Center, Via Santa Maria 67, I-56100 Pisa, Italy. Dr. Pareschi received the "Laurea" in physics from the University of Pisa and a special Master's degree in physics at the Scuola Normale Superiore of Pisa in 1978. In 1979 she received a fellowship at ENEA (Ente Nazionale Energie Alternative), where she worked on problems of plasma physics in collaboration with EURATOM; she later received a grant from the Massachusetts Institute of Technology for studies in computational plasma physics. Dr. Pareschi has been working since 1980 at the IBM Scientific Center at Pisa in the area of modeling and image processing, and has written numerous papers in those fields. In 1989 and 1990 she presented a course on numerical simulation at the Department of Earth Science of Pisa University. Dr. Pareschi is a member of AEEI (Associazione Eletrotecnica e Elletronica Italiana), IAVCEI (International Association of Volcanology and Chemistry of the Earth's Interior), and the Institute of Electrical and Electronics Engineers.

Roberto Santacroce University of Pisa, Department of Earth Science, Via Santa Maria 53, I-56100 Pisa, Italy. Dr. Santacroce received the Doctoral Degree in geophysical science at the University of Pisa in 1968, and has been an assistant professor, associate professor, and, since 1986, professor of volcanology at the University. From 1986 to 1990 he was Director of the International Institute of Volcanology (IIV), a part of the National Council of Research in Catania, Italy. From 1984 to the present, Dr. Santacroce has been coordinator of the Section on Volcanic Hazard Assessment and Zonation of the National Group on Volcanology (GNV), the scientific institution managing all volcanic research in Italy, and since 1988 he has been a member of the technical-scientific commission "Great Risks," the official consulting organization of the Italian Ministry of Civil Defense for the management of emergencies arising from natural disasters. Dr. Santacroce's scientific activity covers several aspects of volcanology, from the origin of magmas and the relationships between volcanism and tectonics (Italy, East Africa and the Red Sea, the Arabian peninsula, and Central and South America) to geothermics (Italy, Ethiopia, and Central America), to volcanic hazard assessment and zonation (Italy). He is the author of more than 70 scientific papers in national and international journals.